

Cell-sized liposome doublets reveal active cortical tension build up

Joël Lemière^{a,b,c,d}, Matthias Bussonnier^{a,b,c,d}, Timo Betz^{a,b,c}, Cécile Sykes^{a,b,c} & Kevin Carvalho^{a,b,c}

^a Institut Curie, Centre de Recherche, Paris, F-75248 France

^b CNRS, UMR 168, Paris, F-75248 France

^c Sorbonne Universités, UPMC Univ Paris 06, UMR 168, Paris, F-75005 France

^d Univ Paris Diderot, Sorbonne Paris Cité, Paris, F-75205 France

Abstract

Cells are able to generate contractile forces and modulate their shape to fulfill their specific functions. The cell cortex, a thin actin shell bound to the plasma membrane, mediates these essential behaviours. It is the substrate for myosin activity which contributes to cortical tension build up, together with actin dynamics. Here, we dissect the sole effect of myosin II on cortical tension increase with a non-invasive method. Cell-sized biomimetic liposomes are arranged in doublets and covered with a stabilized actin cortex anchored to the membrane. The addition of myosin II minifilaments to this doublet triggers a shape change unambiguously related to cortical-tension increase. Our assay paves the way for a quantification of cortical-tension changes triggered by various actin-associated proteins in a cell-sized system.

Introduction

Cells are highly dynamic and need to change their shape in almost all cellular events spanning from division and motility to tissue remodeling. One of the major components involved in these processes is the contractile actin cytoskeleton arranged in a sub-micrometer thick network linked to the plasma membrane and called the acto-myosin cortex [1]. It drives cell-shape changes as well as cell polarization [2] and governs tissue remodeling [3]–[6]. This cortex insures tension in cells, called cortical tension [7]–[9], where the interactions with the plasma membrane and myosins are the essential modulators for this tension. Micromanipulation of cells allows to measure the cortical tension, which was found to be between 50 and 4000 pN/ μ m depending on cell type, myosin activity and actin dynamics [7], [10]–[12]. Moreover, as shown for cell doublets, cell-cell adhesion is able to modulate cortical tension [13], a mechanism that is involved in cell sorting for tissue formation [14]. Recently, acto-myosin cortices have been reconstructed on supported lipid bilayers [15] and on cell-sized liposomes [16] where those reconstructions allowed to understand how crosslinking, attachment to the membrane, and actin-filament length influence contraction by myosin activity and actin polymerization [17].

In this study, we determine cortical-tension changes by the use of cell-sized doublet liposomes around which an acto-myosin cortex is reproduced *in vitro*. Changes in cortical tension are quantified by analyzing doublet-shape change. This approach is reminiscent of cell-cell doublets used to uncover the role of cell adhesion in cortical-tension change [14]. Our assay allows isolating the role of myosin motors on cortical-tension build up, independently of actin dynamics and membrane tension.

Results

Formation of liposome doublets

Liposomes are obtained by electroformation [18] from a mixture of egg-phosphatidylcholine (EPC) and biotin-PEG lipids (**See Material and methods**). We take the advantage of biotin PEG lipids to stick liposomes together by adding streptavidin to the liposome solution (**see MM**). In these conditions, several doublets are formed within 15 minutes (**Fig 1A**).

Attachment of actin on doublet liposomes

Phalloidin-stabilized fluorescent actin filaments, obtained in the presence of biotinylated actin monomers, stick to the membrane of the preformed doublets through a biotin-streptavidin-biotin link (**Fig 1B**) and form a crosslinked homogeneous coat, as already characterized on liposomes [16]. Note that the interface between the two liposomes is free of actin filaments (**Fig 1C - i**). To avoid the use of fluorescent lipids that may affect membrane mechanics [19], this interface is visualized by fluorescently labeling the inside buffer of only one of the liposomes with 0.9 μ M of sulforhodamin B (SRB) (**see MM and Fig 1C - i**).

Effect of myosin injection

Myosin II motors, which assemble into bipolar filaments, are injected in the observation chamber by exchanging the external solution using an H-shaped flow chamber where doublets are imaged (**Fig 1C - ii**). Myosin II motors trigger a shape change of the doublets within minutes (**Fig 1C - iii**) and the following geometrical characteristics of the liposome doublets are modified: the distance between liposome centers (d), the radii R_1 and R_2 of the liposomes 1 and 2, respectively ($R_1 > R_2$), the

radius of curvature of the interface R_i , the volume of the doublet V , the angles between the interface and the liposome 1 or 2, θ_1 and θ_2 respectively. We define the total contact angle $\theta_{tot}=\theta_1+\theta_2$ (**Fig 1D**). These parameters are geometrically linked (**Fig 1D**), and obtained by adjusting two spherical caps in contact, either in 2D-(phase contrast and epifluorescence) images or 3D-(spinning disk) stacks (**see MM**). We use the total contact angle θ_{tot} as a reporter for shape change. We find that myosin addition produces an increase of θ_{tot} . Indeed, on epifluorescence images and in the absence of myosin, we measure a total contact angle θ_{tot} of $(64 \pm 16)^\circ$ ($n=18$) whereas in the presence of 200 nM myosin and before the actin cortex ruptures, we find a θ_{tot} value of $(86 \pm 21)^\circ$ ($n=5$). This difference is statistically significant ($p=0.0186$)

Angles are related to tensions

Liposomes 1 and 2 have a uniform tension τ_1 and τ_2 , respectively. Tension refers to the sole membrane tension in the absence of actin and myosin, and to cortical tension in the presence of actin and myosin. The tension at the interface between liposome 1 and 2 has two components: a membrane tension τ_i and the adhesion energy per unit surface W which is due to biotin-streptavidin-biotin adhesion, and reads $(\tau_i - W)$. The Young's equation, which relates tensions and angles, can be applied to the contact line between the two doublet liposomes (**Fig 1D**). When projected on the contact surface tangent, the Young's equation reads:

$$\tau_i - W = \tau_1 \cos \theta_1 + \tau_2 \cos \theta_2 \quad (1)$$

When projected orthogonally to the contact surface tangent, one finds:

$$\tau_1 \sin \theta_1 = \tau_2 \sin \theta_2 \quad (2)$$

Contact-angle dispersion

Dispersion in θ_{tot} , in a population of doublets before myosin injection is $\pm 16^\circ$. It reflects a difference in tension, which could be due either to the dispersion of tension during the liposome preparation, to a difference in adhesion at the interface between doublet liposomes, or to contribution of the actin shell in tension build up. Contact angle increase upon myosin addition is on the same order of this dispersion, which prompted us to characterize many individual doublets as a function of time.

The sole presence of an actin shell does not modify the contact angle

We now investigate how the actin shell affects the contact angle, and thus the tension, in the absence of myosin. We compare the shape of the same doublet in the presence or in the absence of an actin shell by photo-damaging the actin filamentous network (**Fig 2A**) [20]. The total contact angle changes only by $(3.4 \pm 2)^\circ$ ($n = 7$), (**Fig 2B**) which is negligible compared to the change due to myosin activity (see above).

3D observations

Since the liposomes forming the doublets have size ratios R_1/R_2 that vary between 1.15 and 1.82, the plane of epifluorescence images is generally not parallel to the doublet equatorial plane, hence leading to an underestimate of the angle θ_{tot} . Therefore, 3D spinning disk image stacks are recorded (**Fig 3A**) for an accurate determination of θ_{tot} , V and d (see above for definition) which are obtained by fitting spherical caps on 3D stacks (**see mat and meth**). All initial values before myosin

addition are noted θ_{tot}^I , V^I , d^I and $\theta_{tot}(t)$, $V(t)$, $d(t)$ after addition of myosin at $t=0$. We observe that $\theta_{tot}(t)$ increases, whereas $d(t)$ decreases when myosin filaments are added. During these geometric changes, the volume remains constant within 10% consistent with cell doublet experiments [14], [21] (**Fig 3D**).

Visual inspection of our images reveals that the interface between liposome 1 and 2 only differs from a flat interface by a few pixels (**Fig SI**). The curvature $1/R_i$ (**Fig 1D**) is generally much smaller than $1/R_1$ and $1/R_2$, which are comparable. This observation leads to the assumption that $\theta_1 = \theta_2 = \theta$ within our resolution.

Discussion

Cortical tension is homogeneous for a single doublet

The use of **equation (2)** with $\theta_1(t) = \theta_2(t) = \theta_{tot}(t)/2$ leads to the equality of tensions on both sides of the doublet, thus, $\tau_1(t) = \tau_2(t) = \tau(t)$. This result is consistent with the fact that actin is distributed continuously all around the liposome doublet. Thus, myosin II mini-filaments contract a continuous shell. Under these conditions, **equation (1)** simplifies to:

$$\tau_i - W = 2\tau(t) \cdot \cos \theta(t) \quad (3)$$

Where $\theta(t) = \frac{\theta_{tot}(t)}{2}$ with a reasonable assumption that $\tau_i - W$ may depend on the variability of initial adhesion in our experiments, but is considered constant over time for a given doublet. Therefore, we obtain an expression of the tension $\tau(t)$ that varies during acto-myosin contraction and reads

$$\tau(t) = \frac{\text{cst}}{2 \cdot \cos \theta(t)} \quad (4)$$

Therefore, the tension relative to its initial value over time reads:

$$\frac{\tau(t)}{\tau^I} = \frac{\cos \theta^I}{\cos \theta(t)} \quad (5)$$

Relative increase of cortical tension

Interaction of myosin II filaments with a biomimetic actin cortex induces tension build up. The cortical tension, normalized to its initial value $\frac{\tau(t)}{\tau^I}$, increases and reaches a maximal value $\frac{\tau^{max}}{\tau^I}$ (**Fig 3E**). Note that if the actomyosin shell breaks and peels, the doublet recovers its initial shape (**see dashed blue line for d and θ Fig3**). The relative maximal change in tension is found to be $\frac{\tau^{max}}{\tau^I} = 1.56 \pm 0.56$ (n=5) in 3D and $\frac{\tau^{max}}{\tau^I} = 1.25 \pm 0.15$ (n=5) in epifluorescence, in agreement with the expected underestimates of the contact angle in epifluorescence (see above).

Cortical tension increase in doublets and in cells

In cells, cortical tension can be as low as 50 pN/ μ m in fibroblast progenitor cells [10] and can go up to 4000 pN/ μ m for dictyostelium [11]. Surprisingly, when myosin activity is affected, either by drugs or by genetic manipulation the cortical tension only decreases by a factor of about 2 [7], [10], [11], [22]. Our *in vitro* reconstruction is able to capture this feature in the change of cortical tension. Indeed, we observe the cortical tension of the doublets to increase by a factor 1.1 to 2.4.

Different contributions for cortical tension

Cortical tension is the sum of the membrane tension and the tension due to the actomyosin cortex. In our assay, membrane contributes about 50% to the cortical

tension. In suspended fibroblast cells however, membrane tension is estimated to be only 10% of the cortical tension [7]. This difference may be explained by the absence of actin dynamics in our assay. Actin dynamics is confirmed to have a role on cortical tension that is multiplied by a factor of 5 when polymerization of actin is stimulated [7], [13]. How actin polymerization contributes to cortical tension is still an open question that needs to be addressed in the geometry of the cell. Whereas actin polymerization outside a liposome has been clearly shown to generate inward pressure, is not yet clear how this can be translated into tension in a different geometry. *In vitro* assays are on their way to mimic actin dynamics in cells [23], [24] and will allow unveiling the mechanism of tension build up by actin dynamics. This is the remaining module that needs to be understood, while the effect of myosin is distinguish from the one of membrane in this study.

Conclusion

We provide a biomimetic reconstitution of tension build up through actomyosin contractility using liposome doublets. Cortical tension is visualized *in situ* over time by analyzing doublet shape changes. This method allows us to directly quantify the relative increase in tension due to myosin, separately from the one due to actin dynamics. Understanding contraction of composite systems built brick by brick on the model of a cell tile the road for the reconstitution of complex systems like tissues.

Acknowledgments: This work was supported by the French Agence Nationale pour la Recherche (ANR), grant ANR 09BLAN0283, ANR 12BSV5001401 and ANR-11-JSV5-0002, and by the Fondation pour la Recherche Médicale (FRM), grant

DEQ20120323737. We thank Dr Agnieszka Kawska at IlluScientia for schemes. JL and MB thank the AXA Research Fund for doctoral fellowships. JL and KC were also supported by la Fondation ARC pour la recherche sur le cancer. We thank Thomas Risler and Clément Campillo for critical reading of the manuscript

Material and methods.

Lipids, reagents and proteins. Chemicals are purchased from Sigma Aldrich (St. Louis, MO, USA) unless specified otherwise. L-alpha-phosphatidylcholine (EPC) and 1,2-distearoyl-sn-glycero-3-phosphoethanolamine-N-[biotinyl polyethylene glycol 2000] (biotinylated lipids), 1,2-dioleoyl-sn-glycero-3-phosphocholine are purchased from Avanti polar lipids (Alabaster, USA). Actin and biotinylated actin are purchased from Cytoskeleton (Denver, USA) and used with no further purification. Fluorescent Alexa-488 actin is obtained from Molecular Probes. Monomeric actin containing 10% or 20% of labeled Alexa-488 actin and 0.25% of biotinylated actin is diluted in G-Buffer (2mM Tris, 0.2mM CaCl₂, 0.2mM DTT at pH 8.0). Myosin II is purified from rabbit skeletal muscle and fluorescent myosin II is prepared as previously described [25] and its functionality is confirmed by motility assays showing an average gliding speed of $4.5 \pm 1.5 \mu\text{m/s}$ ($N = 27$) [26]. The working buffer contains 25 mM imidazole, 50 mM KCl, 70 mM sucrose, 1mM Tris, 2 mM MgCl₂, 1 mM ATP, 0.1 mM DTT, 0.02 mg/ml β -casein, adjusted to pH 7.4. All proteins are mixed in the working buffer and myosin II forms minifilaments of approximately 0.7 micrometer length with about 100 motors [27].

Formation of liposome doublets, actin cortices on doublets. Liposomes are electroformed [18]. Briefly, 20 µL of a mixture of EPC lipids and biotin PEG lipids present at 0.1 molar ratio with a concentration of 2.5 mg/ml in chloroform/methanol 5:3 (v:v) are spread on ITO-coated plates and dried under nitrogen flow, then placed under vacuum for 2 hours. A chamber is formed using the ITO plates (their conductive sides facing each other) filled with sucrose buffer (200mM sucrose, 2mM Tris adjusted at pH 7.4, containing or not sulforhodamin B 0.9 µM), and sealed with hematocrit paste (Vitrex medical, Denmark). Liposomes are formed by applying an alternate current voltage (1V - 10 Hz) for 1hour and 15 minutes. Then liposomes are incubated with 160 nM streptavidin for 15 min and diluted 30 times. Note that for the observation of the interface between the doublet liposomes, we prepare separately liposomes in the presence or in the absence of sulforhodamin B, and mix them at equal volume before incubation with streptavidin. At this stage we have doublets coated with streptavidin. Waiting more than 15 min would increase the quantity of liposome aggregates and decrease the quantity of doublets and single liposomes. A bulk solution of 40 µM actin monomers (Cytoskeleton, Denver USA) containing 10% fluorescently labeled actin and 1/400 biotinylated actin monomers is polymerized at 1 µM by diluting 40 times in the working buffer (25 mM imidazole, 50 mM KCl, 70 mM sucrose, 1mM Tris, 2 mM MgCl₂, 1 mM ATP, 0.1 mM DTT, 0.02 mg/ml β-casein, adjusted at a pH 7.4) for 1 hour in the presence of 1 µM of phalloidin (to prevent depolymerization). Actin filaments are then diluted 10-fold to 0.1 µM, mixed with streptavidin-coated doublets of liposomes, and incubated for 15 min. The mix is diluted 5 times for observation to reduce background fluorescence from actin filaments.

Observation chamber design, formation and myosin II injection. Observation chambers are made by heating Parafilm stripes (as spacer) with an H-shape between two coverslips. The solution containing doublets is injected in the chamber and let few minutes in order to let the doublets sediment (**Fig 1C**). Then myosin II filaments are injected in the chamber and the H-shape and doublets are imaged over time in the middle of the chamber (**Fig 1C**). Conditions (streptavidin, actin filament length) are the same as in [16] but observations are made before breakage of the acto-myosin shell.

Observation of doublets. Epifluorescence and phase contrast microscopy are performed using an IX70 Olympus inverted microscope with a 100x or a 60x oil-immersion objective. Spinning-disk confocal microscopy is performed on a Nikon Eclipse T1 microscope with an Andor Evolution Spinning Disc system and a 60x water immersion objective and a z distance of xx μm between z-slices.

Image processing and data analysis. 2D- images: the contact angle is measured by adjusting two circles on binarized liposome images taken by phase contrast or epifluorescence microscopy. 3D-images: The geometrical parameters of the doublets are determined by optimizing the correlation between simulated and acquired 3D recording. Simulated 3D stacks, using [Python], [Numpy] and [Cython] are obtained by creating two spherical caps in contact and reproducing the fluorescent signal of actin at the external surface. Optimizing the correlation between simulated and acquired data is done using [Python] and [SciPy] (Nelder–Mead simplex method from the "optimize" submodule). Initial fit parameters of the first frame of each timelapse are determined visually. For the subsequent frame, we use the optimized parameters as initial parameters. Robustness of fit is checked by several repeats while changing the initial fit parameters by a random amount drawn from a normal distribution (mean

$0\mu\text{m}$ and standard deviation $0.5\mu\text{m}$). The obtained eight parameters (2 centers with X,Y,Z coordinate and 2 liposomes radii) geometrically define the contact angle and the distance between centers. All the data processing was done in an [IPython] environment.

Bibliography

- [1] A. G. Clark, K. Dierkes, E. K. Paluch, « Monitoring Actin Cortex Thickness in Live Cells », *Biophys. J.*, vol. 105, n° 3, p. 570-580, 2013.
- [2] G. Salbreux, G. Charras, E. Paluch, « Actin cortex mechanics and cellular morphogenesis », *Trends Cell Biol.*, 2012.
- [3] E. Munro, J. Nance, J. R. Priess, « Cortical flows powered by asymmetrical contraction transport PAR proteins to establish and maintain anterior-posterior polarity in the early *C. elegans* embryo », *Dev. Cell*, vol. 7, n° 3, p. 413-424, 2004.
- [4] T. Lecuit, P.-F. Lenne, « Cell surface mechanics and the control of cell shape, tissue patterns and morphogenesis », *Nat. Rev. Mol. Cell Biol.*, vol. 8, n° 8, p. 633-644, 2007.
- [5] M. Rauzi, P.-F. Lenne, T. Lecuit, « Planar polarized actomyosin contractile flows control epithelial junction remodelling », *Nature*, vol. 468, n° 7327, p. 1110-1114, 2010.
- [6] M. Rauzi P.-F. Lenne, « Cortical forces in cell shape changes and tissue morphogenesis », *Curr. Top. Dev. Biol.*, vol. 95, p. 93-144, 2011.
- [7] J.-Y. Tinevez, U. Schulze, G. Salbreux, J. Roensch, J.-F. Joanny, E. Paluch, « Role of cortical tension in bleb growth », *Proc. Natl. Acad. Sci. U. S. A.*, vol. 106, n° 44, p. 18581-18586, 2009.
- [8] R. Nambiar, R. E. McConnell, M. J. Tyska, « Control of cell membrane tension by myosin-I », *Proc Natl Acad Sci U S A*, vol. 106, n° 29, p. 11972-11977, 2009.
- [9] D. Raucher, T. Stauffer, W. Chen, K. Shen, S. Guo, J. D. York, M. P. Sheetz, T. Meyer, « Phosphatidylinositol 4,5-bisphosphate functions as a second messenger that regulates cytoskeleton-plasma membrane adhesion », *Cell*, vol. 100, n° 2, p. 221-228, 2000.

- [10] M. Krieg, Y. Arboleda-Estudillo, P.-H. Puech, J. Käfer, F. Graner, D. J. Müller, C.-P. Heisenberg, « Tensile forces govern germ-layer organization in zebrafish », *Nat. Cell Biol.*, vol. 10, n° 4, p. 429-436, 2008.
- [11] E. C. Schwarz, E. M. Neuhaus, C. Kistler, A. W. Henkel, T. Soldati, « Dictyostelium myosin IK is involved in the maintenance of cortical tension and affects motility and phagocytosis », *J. Cell Sci.*, vol. 113 (Pt 4), p. 621-633, 2000.
- [12] T. Luo, K. Mohan, P. A. Iglesias, D. N. Robinson, « Molecular mechanisms of cellular mechanosensing », *Nat. Mater.*, vol. 12, n° 11, p. 1064-1071, 2013.
- [13] W. Engl, B. Arasi, L. L. Yap, J-P. Thiery, V. Viasnoff, « Actin dynamics modulate mechanosensitive immobilization of E-cadherin at adherens junctions », *Nat. Cell Biol.*, vol. 16, n° 6, p. 587-594, 2014.
- [14] J.-L. Maître, H. Berthoumieux, S. F. G. Krens, G. Salbreux, F. Jülicher, E. Paluch, C.-P. Heisenberg, « Adhesion Functions in Cell Sorting by Mechanically Coupling the Cortices of Adhering Cells », *Science*, vol. 338, n° 6104, p. 253-256, 2012.
- [15] M. P. Murrell M. L. Gardel, « F-actin buckling coordinates contractility and severing in a biomimetic actomyosin cortex », *Proc. Natl. Acad. Sci.*, 2012.
- [16] K. Carvalho, F. C. Tsai, E. Lees, R. Voituriez, G. H. Koenderink, C. Sykes, « Cell-sized liposomes reveal how actomyosin cortical tension drives shape change », *Proc. Natl. Acad. Sci.*, 2013.
- [17] K. Carvalho, J. Lemière, F. Faqir, J. Manzi, L. Blanchoin, J. Plastino, T. Betz, C. Sykes, « Actin polymerization or myosin contraction: two ways to build up cortical tension for symmetry breaking », *Philos. Trans. R. Soc. B Biol. Sci.*, vol. 368, n° 1629, 2013.
- [18] M. Angelova, D. Dimitrov, « Liposome electroformation », *Faraday Discuss.*, vol. 81, p. 303+, 1986.
- [19] O. Sandre, L. Moreaux, F. Brochard-Wyart, « Dynamics of transient pores in stretched vesicles », *Proc. Natl. Acad. Sci. U. S. A.*, vol. 96, n° 19, p. 10591-10596, 1999.
- [20] J. van der Gucht, E. Paluch, J. Plastino, C. Sykes, « Stress release drives symmetry breaking for actin-based movement », *Proc. Natl. Acad. Sci. U. S. A.*, vol. 102, n° 22, p. 7847-7852, 2005.

- [21] J. Sedzinski, M. Biro, A. Oswald, J.-Y. Tinevez, G. Salbreux, E. Paluch, « Polar actomyosin contractility destabilizes the position of the cytokinetic furrow », *Nature*, vol. 476, n° 7361, p. 462-466, 2011.
- [22] P. Kunda, A. E. Pelling, T. Liu, B. Baum, « Moesin controls cortical rigidity, cell rounding, and spindle morphogenesis during mitosis », *Curr. Biol. CB*, vol. 18, n° 2, p. 91-101, 2008.
- [23] E. Abu Shah, K. Keren, « Symmetry breaking in reconstituted actin cortices », *eLife*, vol. 3, p. e01433, 2014.
- [24] T. Luo, V. Srivastava, Y. Ren, D. N. Robinson, « Mimicking the mechanical properties of the cell cortex by the self-assembly of an actin cortex in vesicles », *Appl. Phys. Lett.*, vol. 104, n° 15, p. 153701, 2014.
- [25] G. H. Koenderink, Z. Dogic, F. Nakamura, P. M. Bendix, F. C. MacKintosh, J. H. Hartwig, T. P. Stossel, D. A. Weitz, « An active biopolymer network controlled by molecular motors », *Proc. Natl. Acad. Sci. U. S. A.*, vol. 106, n° 36, p. 15192-15197, 2009.
- [26] Y. Y. Toyoshima, S. J. Kron, E. M. McNally, K. R. Niebling, C. Toyoshima, J. A. Spudich, « Myosin subfragment-1 is sufficient to move actin filaments in vitro », *Nature*, vol. 328, n° 6130, p. 536-539, 1987.
- [27] M. S. E. Silva, M. Depken, B. Stuurmann, M. Korsten, F. C. Mackintosh, G. H. Koenderink, « Active multistage coarsening of actin networks driven by myosin motors », *Proc. Natl. Acad. Sci. U. S. A.*, 2011.

Figure 1

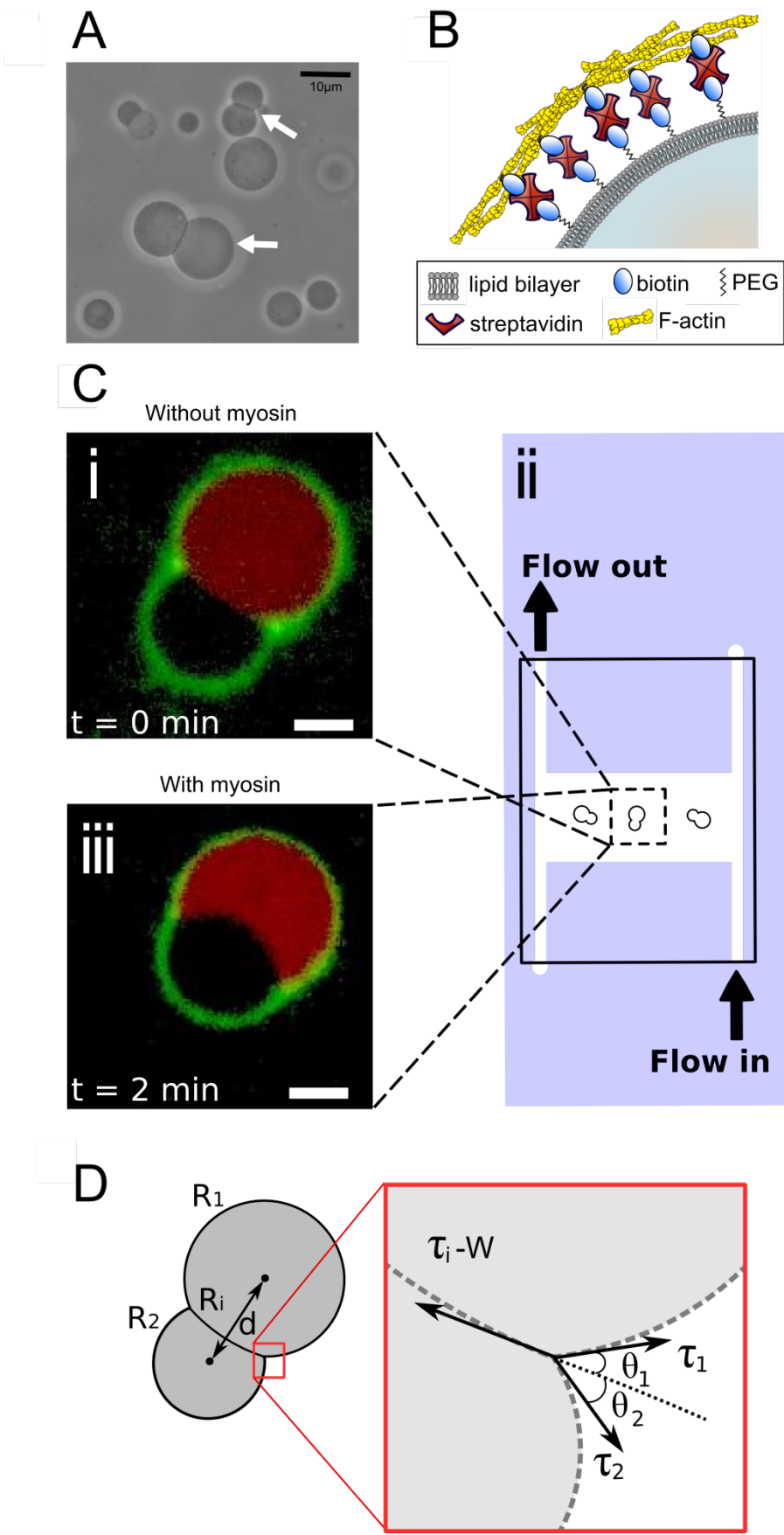
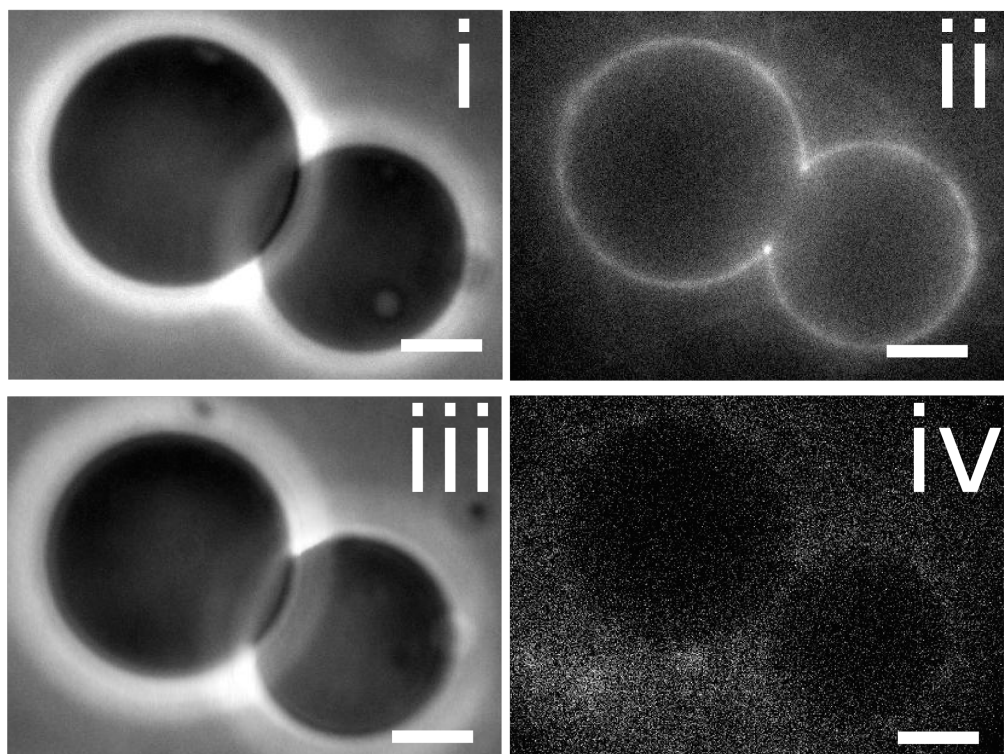


Figure 2

A



B

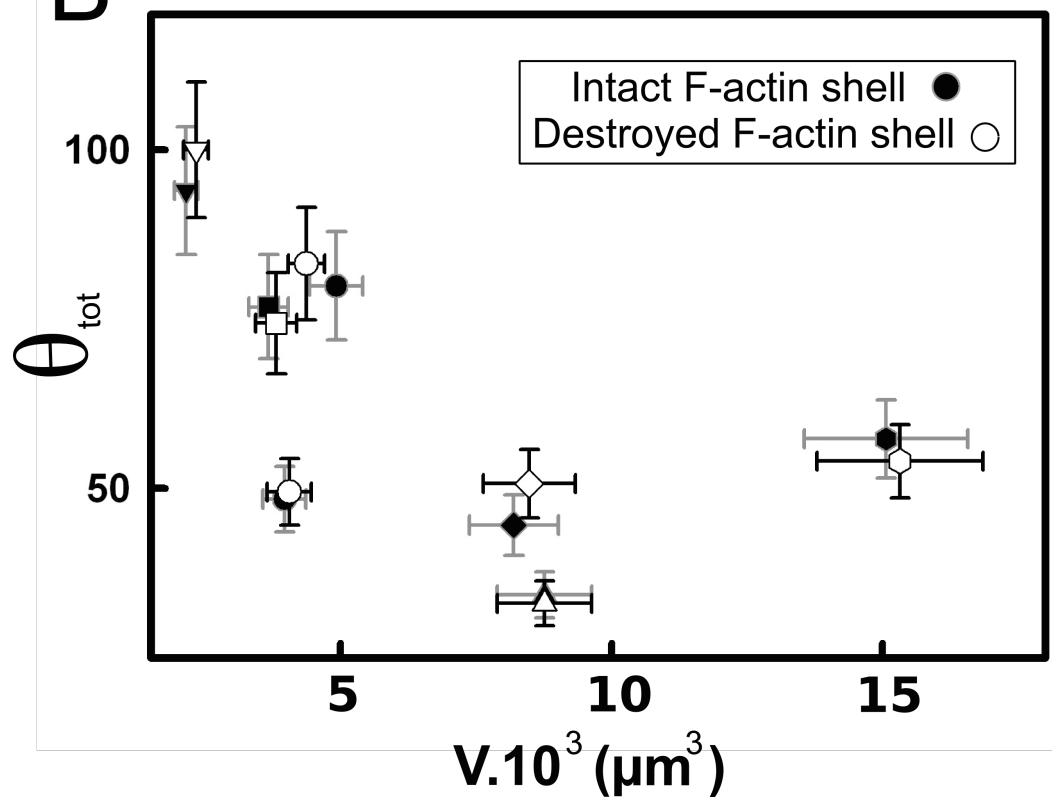
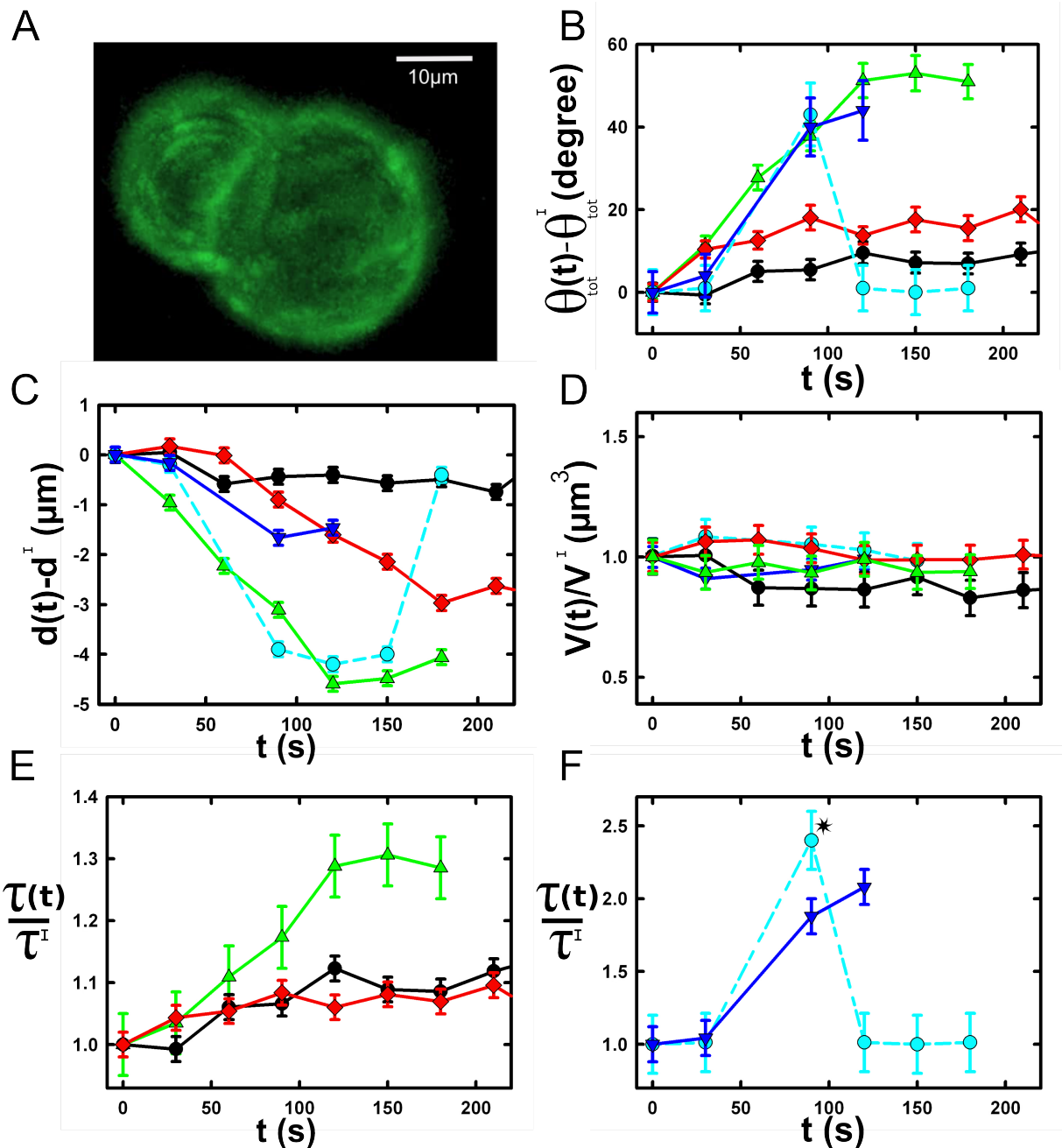


Figure 3



Supplementary figure

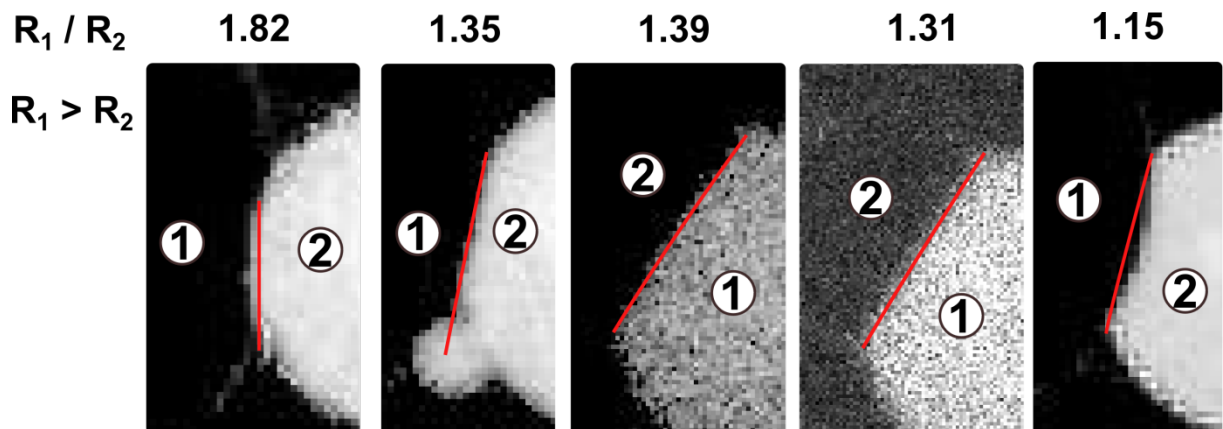
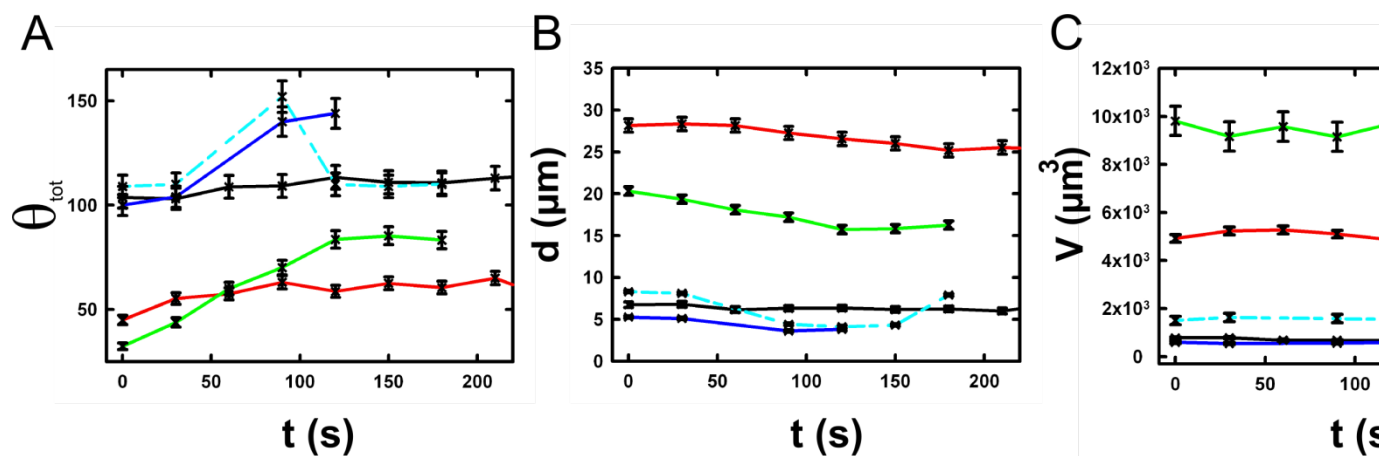


Figure Captions

Figure 1: Cell-sized liposome doublets. A) Doublets, indicated by white arrows, in the field of view of a phase contrast microscope. B) Schematic of the stabilized actin cortex at the membrane (proteins not to scale). C) ii) Macrofluidics chamber designed to exchange the outside buffer. Doublets are visualized in the middle horizontal channel of the H shape chamber to avoid movement during the buffer exchange. Spinning disk images of the doublet before i) or after iii) myosin II injection. One liposome contains SRB (red) to visualize the interface of the doublet, the actin cortex is labeled in green. Scale bar 5 μ m. D) Simplification of the doublet with the three characteristic radii. Inset: enlargement of the contact interface between the two liposomes with the Young's tension vector and the contact angle.

Figure 2: Effect of an actin cortex on the doublet's shape. A) Image of the same doublet coated with fluorescent actin before i) ii) and after iii) iv) actin cortex disruption. The actin cortex is visualized by epifluorescence ii) iv) and the doublet by phase contrast i) iii). Scale bar 5 μ m. B) Measurement of the contact angle between the two liposomes as a function of their volume, before (black) and after (white) disruption of the stabilized actin cortex.

Figure 3: Geometrical parameters over time: A) 3D reconstruction of a doublet surrounded by actin. Note that there is no actin at the interface between the liposomes. B) Evolution of the contact angle compare to the initial one as a function of time. Each doublet is represented by a different line color. C) Evolution of the

distance between the two liposomes center over time. D) Evolution of the volume ratio over time. E) Increase of the tension ratio between the tension $\tau(t)$ at time t and the initial one τ^I . Note that the blue dashed line A-B-C-D) corresponds to the evolution of geometrical parameters of the same doublet, analyzed even after actin cortex rupture. It recovers its initial parameter values.